



Cite this: *Dalton Trans.*, 2022, 51, 11226

Received 18th May 2022,  
Accepted 28th June 2022

DOI: 10.1039/d2dt01553f

rsc.li/dalton

## A cavity-shaped *cis*-chelating P,N ligand for highly selective nickel-catalysed ethylene dimerisation†

Yang Li,<sup>a</sup> Katrin Pelzer,<sup>a</sup> Damien Sechet,<sup>b</sup> Geordie Creste,<sup>a</sup> Dominique Matt,<sup>b</sup> Pierre Braunstein<sup>b</sup>\*<sup>a</sup> and Dominique Armspach<sup>b</sup>\*<sup>a</sup>

The presence of a permethylated  $\alpha$ -cyclodextrin ( $\alpha$ -CD) cavity in a chelating P,N ligand promotes exclusive formation of 1 : 1 ligand/metal complexes. In  $\text{MX}_2$  complexes, one of the two halido ligands is forced to reside inside the CD hollow while the second one is pointing outside. Unlike its cavity-free analogue, a Ni(II) complex of the CD ligand is a highly selective precatalyst for ethylene dimerisation (96%  $\text{C}_4$  selectivity with up to 95% of 1-butene within the  $\text{C}_4$  fraction).

Inwardly directed donor atoms rigidly grafted on a macrocyclic host molecule are capable of facilitating a metal centred reaction to take place inside the cavity-shaped ligand.<sup>1–5</sup> This feature is prone to produce high substrate recognition,<sup>6–14</sup> catalytic chemo-<sup>15</sup> and regioselectivity<sup>16–20</sup> as well as enantioselectivity if the receptor is optically active.<sup>21</sup> By connecting two C-6 carbon atoms of two glucose units of an  $\alpha$ -,  $\beta$ - or  $\gamma$ -CD with a single donor atom such as nitrogen<sup>22</sup> or phosphorus,<sup>23–25</sup> (Fig. 1i) or a short NHC unit<sup>26–28</sup> (Fig. 1ii), it was previously shown that the resulting bridge is sufficiently rigid to force the donor atom lone pair to point towards the CD interior. Doubly bridged ligands with a similar metal confining feature have also been prepared (Fig. 1iii).<sup>23,24</sup> Almost all ligands of that type are monodentate or *trans*-chelating bidentate. However, most metal-catalysed reactions involve *cis*-chelate complexes. Increasing the structural diversity of *cis*-chelating ligands displaying a metal confining unit<sup>22,29–31</sup> would considerably widen the scope of metal binding host molecules, in particular if catalytically relevant P(III) atoms

could be incorporated into the macrocyclic structure. Self-assembled, *cis*-chelating P,N ligands consisting of a water-soluble phosphine ligand included in a mono-*N,N*-dialkyl-amino- $\beta$ -CD were already prepared in water, but in these complexes, the metal centre is not located in the CD cavity.<sup>32,33</sup>

Herein, we describe a rare example of P(III)-containing CD (1) capable of forcing the exclusive formation of a 1 : 1 ligand/metal complex, showing *cis*-chelation inside the receptor hollow when associated with a N donor atom. A Ni(II) complex of this new P,N ligand was investigated for its potential as precatalyst in ethylene oligomerisation, a reaction of continuing considerable interest<sup>34,35</sup> and its properties were compared to those of a cavity-free analogue.

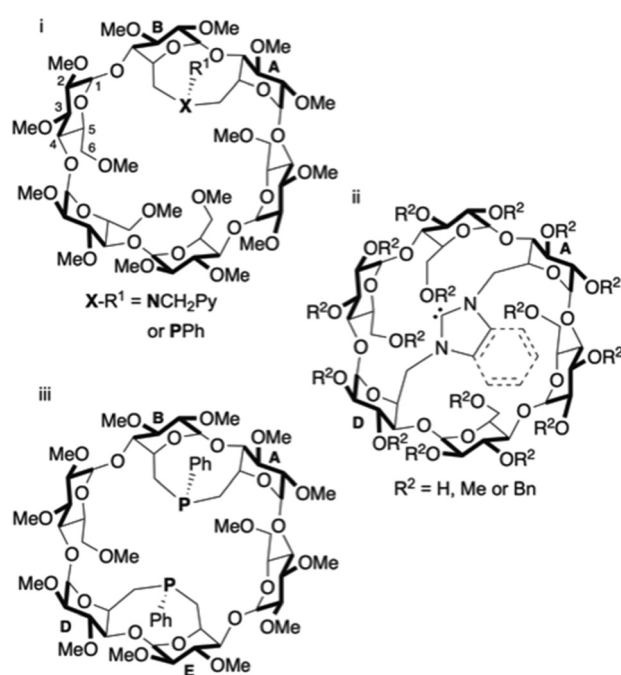


Fig. 1 Examples of  $\alpha$ -CD-based metal confining ligands with one (i and ii) or two (iii) bridging coordinating units. Bn stands for benzyl.

<sup>a</sup>Equipe Confinement Moléculaire et Catalyse, Institut de Chimie de Strasbourg, UMR 7177 CNRS, Université de Strasbourg, 4, rue Blaise Pascal, CS 90032, 67081 Strasbourg Cedex, France. E-mail: d.armspach@unistra.fr

<sup>b</sup>Laboratoire de Chimie Inorganique Moléculaire et Catalyse, Institut de Chimie de Strasbourg, UMR 7177 CNRS, Université de Strasbourg, 4, rue Blaise Pascal, CS 90032, 67081 Strasbourg Cedex, France

† Electronic supplementary information (ESI) available: Synthesis and characterization data. CCDC 2163655 (8), 2163663 (9), 2163657 (10), 2163751 (11), 2163658 (12) and 2163666 (13). For ESI and crystallographic data in CIF or other electronic format see DOI: <https://doi.org/10.1039/d2dt01553f>



An improved procedure (Scheme 1) was devised to synthesise diethyl [2-(*N,N*-dimethylamino)phenyl]phosphonate (**3**) from 2-bromoaniline (**2**).<sup>36</sup> Its reduction afforded the key functional primary phosphine **4**, which upon deprotonation reacted with dimesylate **5** to afford P,N ligand **1** in 63% yield. Although **1** is seemingly a very basic phosphine ( $\delta_{31\text{P}} = -28.4$  ppm), this ligand is considerably more stable towards air than its PhP-bridged analogue ( $\delta_{31\text{P}} = -16.2$  ppm)<sup>23</sup> and can be purified by standard column chromatography without noticeable formation of phosphine oxide. For comparison, the related cavity-free ligand **7**<sup>37</sup> was also synthesised in 40% yield from 2-bromo-*N,N*-dimethylaniline by *ortho*-lithiation followed by nucleophilic substitution of chlorodiethylphosphine.<sup>38</sup> Resistance to oxidation was also observed for **7** ( $\delta_{31\text{P}} = -25.1$  ppm) as in analogous P,N ligands of the Me-DalPhos family (Fig. 2).<sup>39</sup>

When reacted with [PdCl<sub>2</sub>(cod)] (cod = 1,5-cyclooctadiene) in CH<sub>2</sub>Cl<sub>2</sub>, confining ligand **1** produced only chelate complex **8**, even in the presence of excess ligand (Fig. S80†). Chelating behaviour was also observed when **1** or the cavity-free **7** were reacted with [NiBr<sub>2</sub>(dme)] (dme = 1,2-dimethoxymethane) to produce complexes **9** and **10**, respectively.<sup>40</sup> In stark contrast, the reaction of **7** with one equiv. of [PdCl<sub>2</sub>(cod)] in CH<sub>2</sub>Cl<sub>2</sub> gave a 9 : 1 mixture of the chelate complex **11** and the cationic bis(phosphine) complex **12**, respectively. As expected, raising the ligand/metal ratio to 2 : 1 caused the proportion of complex **12**



**Scheme 1** Synthesis of the confining ligand **1** and its cavity-free analogue **7**. Ms stands for methylsulfonyl.

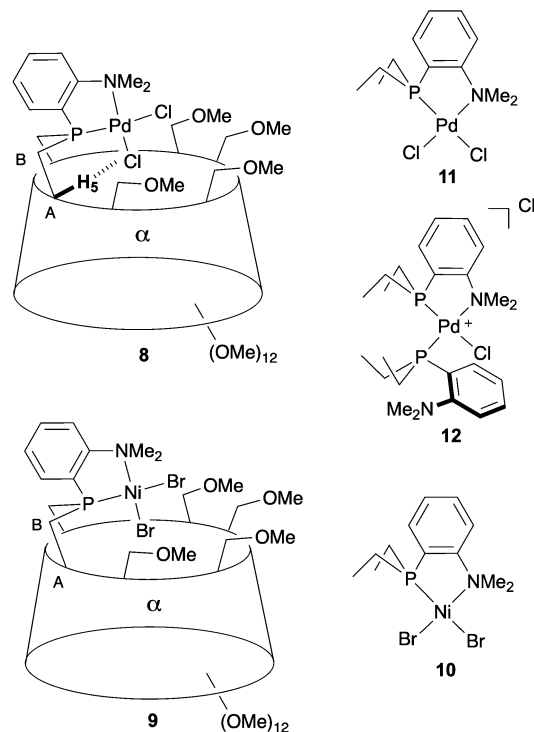


**Fig. 2** Cavity-shaped Pd and Ni chelate complexes **8** and **9**, their cavity-free counterparts **11** and **10**, and cationic Pd complex **12**.

to increase significantly (**11/12** ratio of 3 : 7) (Fig. S80†). The structures of both **11** and **12** were established by X-ray diffraction analyses (Fig. 3). The single crystal X-ray structure of cationic **12** clearly shows that two phosphines but only one tertiary amine are coordinated to palladium (Fig. 3). Furthermore, line broadening upon heating **12** in CDCl<sub>3</sub> (Fig. S66 and S67†) suggests fluxional behaviour possibly involving the slow coordination/decoordination of the NMe<sub>2</sub> units on the NMR time scale (Fig. S1†). Confirmation of the metal confining character of ligand **1** in solution came from a

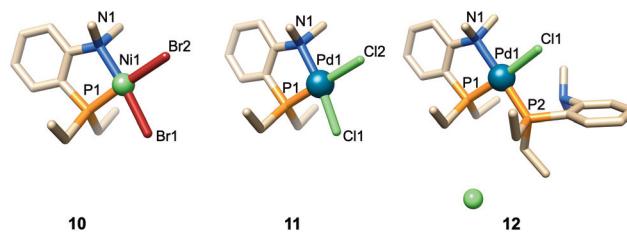


**Fig. 3** Single crystal X-ray structures of cavity-free Pd complexes **11** and **12** as well as Ni complex **10**. Solvent molecules have been omitted for clarity. Selected bond lengths (Å) and angles (°): **10**, Ni1–P1 2.1248(10), Ni1–N1 2.010(3), Ni1–Br1 2.3122(6), Ni1–Br2 2.3626(5); P1–Ni1–N1 88.63(9), P1–Ni1–Br1 85.25(3), N1–Ni1–Br2 94.48(8), Br1–Ni1–Br2 91.64(2); **11**, Pd1–P1 2.1857(9), Pd1–N1 2.111(3), Pd1–Cl1 2.2982(9), Pd1–Cl2 2.4087(9); P1–Pd1–N1 86.68(8), P1–Pd1–Cl1 87.20(3), N1–Pd1–Cl2 94.33(8), Cl1–Pd1–Cl2 91.81(3); **12**, Pd1–P1 2.2326(15), Pd1–P2 2.2724(14), Pd1–N1 2.185(5), Pd1–Cl1 2.3728(14); P1–Pd1–N1 84.71(17), P1–Pd1–P2 95.45(5), N1–Pd1–Cl1 91.36(17), P2–Pd1–Cl1 88.28(5).



detailed analysis of the  $^1\text{H}$  NMR spectrum of the square planar Pd(II) complex **8**, the  $^{31}\text{P}$  NMR chemical shift of which is in the expected range ( $\delta_{31\text{P}} = 32.5$  ppm). As previously reported for a CD-encapsulated M–X unit, the inner-cavity H-5 proton of bridging unit A in **8** is unusually downfield shifted ( $\delta_{\text{H}5} = 5.19$  vs. 4.30 ppm for ligand **1**) as a result of weak  $\text{CH}\cdots\text{Cl}$  H-bonding within the CD hollow. The deshielding of this proton proves that **1** is indeed metal confining in solution. Such a feature was confirmed in the solid state by the single crystal X-ray structure of **8** (Fig. 4), which revealed a square planar  $\text{PdCl}_2$  unit seating just above the cavity and nearly orthogonal to the macrocyclic structure ( $86.05^\circ$ ). $\ddagger$  As expected from the solution studies, one of the two chlorido ligands points toward the interior of the cavity and displays short contact with the H-5 proton of bridging unit A (2.840 Å). The other is clearly pointing outside and is at a much longer distance to palladium (2.368 Å) than the encapsulated one (2.295 Å). This is to be expected because of the larger *trans* influence of the P(III) donor atom. Both complexes **9** and **10** are diamagnetic in keeping with their square planar structures (Fig. 4 and 3 respectively) and low temperature NMR studies in  $\text{CD}_2\text{Cl}_2$  revealed at  $-60$  °C a well-defined  $^{31}\text{P}$  singlet at 10.4 and 41.4 ppm, respectively. $\S$  It is noteworthy that the single crystal X-ray structures of **8** and **9**, which are very similar, clearly

establish that each halido ligand experiences a very different steric environment, an unprecedented feature in metal confining ligands that could have a great impact on catalytic properties. In the Pd complex **8**, the  $\text{PNMX}_2$  unit is slightly more included in the cavity than in its Ni counterpart **9** (angle between CD O-4 atoms and the C6–P1–C16 planes =  $50.27^\circ$  vs.  $54.82^\circ$  respectively). Moreover, both cavity-free and cavity-shaped complexes of  $d^8$  metals have a very similar first coordination sphere, the only significant difference between the two types of complexes being an elongation of the external Ni–Br bond by *ca.* 0.02 Å on going from **10** to **9** and a shortening of the corresponding M–X bond by *ca.* 0.04 Å on going from Pd complexes **11** to **8** (Fig. 3 and 4). The gold(I) complex **13** was also synthesised quantitatively by reacting **1** with  $[\text{AuCl}(\text{tth})]$  (tth = tetrahydrothiophene). Unlike its  $d^8$  counterparts, the  $d^{10}$  metal cation is not chelated by the ligand but only bound to the P(III) atom, leaving the  $\text{NMe}_2$  unit uncoordinated above the encapsulated metal centre, as revealed by its single crystal X-ray structure (Fig. 4). As in monophosphine analogues, $^{23,24}$  the phosphorus donor atom imposes the overall orientation of the metal with respect to the cavity. The steric protection provided by the CD cavity is responsible for a remarkable control of the metal coordination sphere and prevents the formation of bis (phosphine) complexes analogous to **12**. Such a feature is also expected to be retained under catalytic reaction conditions.

Numerous Ni complexes derived from P,N ligands, most of them of the pyridine–phosphine type, $^{41-43}$  have been evaluated in the catalytic oligomerisation of ethylene. $^{44,45}$  Many studies have focused on varying the electronic properties of both P- and N-donor atoms, but steric factors have also been found to play a crucial role in the metal-catalysed oligomerisation of ethylene to  $\alpha$ -olefins. $^{46,54}$  In particular, the presence of steric bulk at the metal axial sites tends to inhibit termination reactions, thus favouring chain growth. $^{47}$  The cavity-shaped complex **9** exhibits a unique steric environment, in which the phosphorus atom is heavily congested and forces the chelated metal to be encapsulated in the CD with both axial sites protected by CD 6-methoxy groups. Moreover, unlike their cavity-free analogues, the two active coordination sites involved in the oligomerisation process, generated by bromide abstraction and methylation of **9**, will experience very different steric environments. While one of the active sites is deeply buried in the CD cavity, the other is much less protected. The unusual steric environment around the metal in Ni complex **9** prompted us to evaluate it as a precatalyst in ethylene oligomerisation. For comparison, the cavity-free analogue **10** was also tested under similar reaction conditions.

After activation with MMAO, the Ni complex **9** catalysed the dimerisation of ethylene with high  $\text{C}_4$  (96%) and 1-butene (95%) selectivities (Table 1, entry 2), even after 24 h reaction time (Table 1, entry 3), indicating that chain-walking and post-isomerisation reactions do not readily take place. Moreover, the proportion of 1-hexene in the small  $\text{C}_6$  fraction is also much higher with the cavity-shaped ligand (70% on average for **9**). Even if such level of selectivity is not uncommon for early transition metals, $^{48}$  it is very high for a nickel-catalysed



**Fig. 4** Single crystal X-ray structures of chelate Pd complex **8** and Ni complex **9**, and monophosphine Au complex **13** displaying metal encapsulation. Solvent molecules have been omitted for clarity. Selected bond lengths (Å) and angles ( $^\circ$ ): **8**, Pd1–P1 2.1947(14), Pd1–N1 2.125(4), Pd1–Cl1 2.2949(14), Pd1–Cl2 2.3676(15); P1–Pd1–N1 86.83(12), P1–Pd1–Cl1 88.49(5), N1–Pd1–Cl2 92.05(12), Cl1–Pd1–Cl2 92.63(6); **9**, Ni1–P1 2.1263(15), Ni1–N1 2.007(6), Ni1–Br1 2.3063(10), Ni1–Br2 2.3807(9); P1–Ni1–N1 88.53(15), P1–Ni1–Br1 84.06(5), N1–Ni1–Br2 95.01(15), Br1–Ni1–Br2 92.40(3); **13**, Au1–P1 2.2329(18), Au1–Cl1 2.2755(19); P1–Au1–Cl1 178.16(7).



**Table 1** Ethylene oligomerisation with nickel complexes **9** and **10** as precatalysts in the presence of MMAO<sup>a</sup>

| Entry | Precatalyst | Time   | Activity [g(C <sub>2</sub> H <sub>4</sub> ) g(Ni) <sup>-1</sup> h <sup>-1</sup> ] | TOF [mol(C <sub>2</sub> H <sub>4</sub> ) mol(Ni) <sup>-1</sup> h <sup>-1</sup> ] | Products weight distribution <sup>b</sup> [%] |                                 |                |
|-------|-------------|--------|---|--|---|---------------------------------|----------------|
|       |             |        |   |  | C <sub>4</sub> (α) <sup>c</sup>               | C <sub>6</sub> (α) <sup>d</sup> | C <sub>8</sub> |
| 1     | <b>9</b>    | 35 min | 2760  | 5780   | 92 (95)                                       | 6 (70)                          | 2              |
| 2     | <b>9</b>    | 3 h    | 2190  | 4580   | 96 (95)                                       | 3 (75)                          | <1             |
| 3     | <b>9</b>    | 24 h   | 1910  | 4000   | 85 (92)                                       | 12 (65)                         | 3              |
| 4     | <b>10</b>   | 35 min | 41 570  | 86 970   | 77 (71)                                       | 22 (8)                          | 1              |
| 5     | <b>10</b>   | 3 h    | 17 920  | 37 490   | 79 (81)                                       | 19 (8)                          | 2              |
| 6     | <b>10</b>   | 24 h   | 5740  | 12 000   | 75 (67)                                       | 24 (6)                          | 1              |

<sup>a</sup> Conditions: amount of catalyst:  $1 \times 10^{-5}$  mol, amount of cocatalyst (MMAO-12):  $4 \times 10^{-3}$  mol (400 equiv.),  $T = 30\text{--}35$  °C, solvent: toluene, total volume: 20 mL, 10 bar C<sub>2</sub>H<sub>4</sub>, every test was repeated at least twice. <sup>b</sup> % calculated by GC analysis. <sup>c</sup> 1-Butene vs. total butenes formed. <sup>d</sup> 1-Hexene vs. total hexenes formed.

reaction.<sup>44,45</sup> For comparison, the related nickel complex **10** (Table 1, entry 4), which has similar electronic properties, but lacks the CD cavity is about 15 times more active for short reaction times, but its activity rapidly drops with time as it is only 3 fold higher than that of **9** after 24 h (Table 1, entry 6). It is much less selective for C<sub>4</sub> (77%) and 1-butene (71%) as well as 1-hexene (8%), whether for short (Table 1, entry 4) or longer reaction times (Table 1, entries 5 and 6). These poor selectivities are also observed for many other P,N Ni complexes except for ligands displaying sterically hindered nitrogen or phosphorus atoms<sup>49,50</sup> Although moderately active (TOF = 5780 mol (C<sub>2</sub>H<sub>4</sub>) mol(Ni)<sup>-1</sup> h<sup>-1</sup>) (Table 1, entry 1), the catalyst derived from **9** proved to be very robust, since loss of activity is marginal over a prolonged period of time in stark contrast with cavity-free **10**. Despite the steric protection of axial positions, which is known to retard the rate of chain transfer relative to chain propagation and improve thermal stability,<sup>47</sup> including in macrocyclic complexes,<sup>51</sup> hardly any C<sub>6</sub>-olefins and higher oligomers were formed. The high selectivity for 1-butene strongly suggests that metal encapsulation in the rather small α-CD cavity does not allow further chain growth and largely prevents isomerisation although the ligand electronic properties as revealed by slight changes in the UV spectra of complexes **8–11** (Fig. S87 and S88†) on going from cavity-free to cavity-shaped systems may also have an impact on the catalytic outcome.<sup>52,53</sup> Further *cis*-chelating and confining ligands with different donor atoms and larger cavities will be tested next in our group to see whether access to longer oligomers with a narrow mass distribution can be achieved. The present study also revealed that encapsulation exclusively leads to complexes with a 1 : 1 ligand/metal ratio, allowing the possibility to introduce in the potentially chelating unit a much weaker donor group susceptible to display catalytically relevant hemilability in solution. This unusual behaviour constitutes a promising development in the design of hybrid functional ligands.

## Conflicts of interest

There are no conflicts to declare.

## Acknowledgements

We thank the China Scholarship Council for a PhD studentship awarded to Y. L. (CSC201808420261).

## Notes and references

‡ Angle between the CD O-4 atoms plane and the 5-membered chelate ring.

§ Line broadening at room temperature is common with this type of complexes.

- R. Gramage-Doria, D. Armspach and D. Matt, *Coord. Chem. Rev.*, 2013, **257**, 776–816.
- S. H. A. M. Leenders, R. Gramage-Doria, B. de Bruin and J. N. H. Reek, *Chem. Soc. Rev.*, 2015, **44**, 433–448.
- V. Mouarrawis, R. Plessius, J. I. van der Vlugt and J. N. H. Reek, *Front. Chem.*, 2018, **6**, 623.
- D. Matt and J. Harrowfield, *ChemCatChem*, 2021, **13**, 153–168.
- G. R. F. Orton, B. S. Pilgrim and N. R. Champness, *Chem. Soc. Rev.*, 2021, **50**, 4411–4431.
- B.-Y. Wang, T. Žujović, D. A. Turner, C. M. Hadad and J. D. Badjić, *J. Org. Chem.*, 2012, **77**, 2675–2688.
- A. Cavarzan, J. N. H. Reek, F. Trentin, A. Scarso and G. Strukul, *Catal. Sci. Technol.*, 2013, **3**, 2898–2901.
- M. Otte, P. F. Kuijpers, O. Troeppner, I. Ivanović-Burmazović, J. N. H. Reek and B. de Bruin, *Chem. – Eur. J.*, 2014, **20**, 4880–4884.
- P. F. Kuijpers, M. Otte, M. Dürr, I. Ivanović-Burmazović, J. N. H. Reek and B. de Bruin, *ACS Catal.*, 2016, **6**, 3106–3112.
- M. Otte, *ACS Catal.*, 2016, **6**, 6491–6510.
- D. Zhang, J.-P. Dutasta, V. Dufaud, L. Guy and A. Martinez, *ACS Catal.*, 2017, **7**, 7340–7345.
- T. Chavagnan, C. Bauder, D. Sémeril, D. Matt and L. Toupet, *Eur. J. Org. Chem.*, 2017, 70–76.
- C. Tugny, N. del Rio, M. Koohgard, N. Vanthuyne, D. Lesage, K. Bijouard, P. Zhang, J. Mejjide Suárez, S. Roland and E. Derat, *ACS Catal.*, 2020, **10**, 5964–5972.
- J. Mejjide Suárez, O. Bistri-Aslanoff, S. Roland and M. Sollogoub, *ChemCatChem*, 2022, **14**, e202101411.



- 15 G. Xu, S. Leloux, P. Zhang, J. Meijide Suárez, Y. Zhang, E. Derat, M. Ménand, O. Bistri-Aslanoff, S. Roland, T. Leysens, O. Riant and M. Sollogoub, *Angew. Chem., Int. Ed.*, 2020, **59**, 7591–7597.
- 16 T. Gadzikwa, R. Bellini, H. L. Dekker and J. N. H. Reek, *J. Am. Chem. Soc.*, 2012, **134**, 2860–2863.
- 17 M. Jouffroy, R. Gramage-Doria, D. Armspach, D. Sémeril, W. Oberhauser, D. Matt and L. Toupet, *Angew. Chem.*, 2014, **126**, 4018–4021.
- 18 C. García-Simón, R. Gramage-Doria, S. Raoufmoghammad, T. Parella, M. Costas, X. Ribas and J. N. Reek, *J. Am. Chem. Soc.*, 2015, **137**, 2680–2687.
- 19 P. Zhang, J. Meijide Suárez, T. Driant, E. Derat, Y. Zhang, M. Ménand, S. Roland and M. Sollogoub, *Angew. Chem., Int. Ed.*, 2017, **56**, 10821–10825.
- 20 N. Endo, M. Inoue and T. Iwasawa, *Eur. J. Org. Chem.*, 2018, 1136–1140.
- 21 Z. Kaya, E. Bentouhami, K. Pelzer and D. Armspach, *Coord. Chem. Rev.*, 2021, **445**, 214066.
- 22 D. Sechet, Z. Kaya, T. A. Phan, M. Jouffroy, E. Bentouhami, D. Armspach, D. Matt and L. Toupet, *Chem. Commun.*, 2017, **53**, 11717–11720.
- 23 E. Engeldinger, L. Poorters, D. Armspach, D. Matt and L. Toupet, *Chem. Commun.*, 2004, 634–635.
- 24 R. Gramage-Doria, D. Rodriguez-Lucena, D. Armspach, C. Egloff, M. Jouffroy, D. Matt and L. Toupet, *Chem. – Eur. J.*, 2011, **17**, 3911–3921.
- 25 M. Jouffroy, D. Armspach and D. Matt, *Dalton Trans.*, 2015, **44**, 12942–12969.
- 26 M. Guitet, P. Zhang, F. Marcelo, C. Tugny, J. Jiménez-Barbero, O. Buriez, C. Amatore, V. Mouriès-Mansuy, J. P. Goddard and L. Fensterbank, *Angew. Chem., Int. Ed.*, 2013, **52**, 7213–7218.
- 27 P. Zhang, C. Tugny, J. Meijide Suárez, M. Guitet, E. Derat, N. Vanthuyne, Y. Zhang, O. Bistri, V. Mouriès-Mansuy, M. Ménand, S. Roland, L. Fensterbank and M. Sollogoub, *Chem*, 2017, **3**, 174–191.
- 28 Z. Kaya, L. Andna, D. Matt, E. Bentouhami, J. P. Djukic and D. Armspach, *Chem. – Eur. J.*, 2018, **24**, 17921–17926.
- 29 I. Tabushi and Y. Kuroda, *J. Am. Chem. Soc.*, 1984, **106**, 4580–4584.
- 30 O. Sénèque, M. Campion, B. Douziech, M. Giorgi, Y. Le Mast and O. Renaud, *Dalton Trans.*, 2003, 4216–4218.
- 31 M. Jouffroy, D. Sémeril, D. Armspach and D. Matt, *Eur. J. Org. Chem.*, 2013, 6069–6077.
- 32 C. Machut, J. Patrigeon, S. Tilloy, H. Bricout, F. Hapiot and E. Monflier, *Angew. Chem., Int. Ed.*, 2007, **46**, 3040–3042.
- 33 J. Patrigeon, F. Hapiot, M. Canipelle, S. Manuel and E. Monflier, *Organometallics*, 2010, **29**, 6668–6674.
- 34 O. L. Sydora, *Organometallics*, 2019, **38**, 997–1010.
- 35 Z. Wang, Q. Liu, G. A. Solan and W.-H. Sun, *Coord. Chem. Rev.*, 2017, **350**, 68–83.
- 36 F. Y. Xu, O. M. Duke, D. Rojas, H. M. Eichelberger, R. S. Kim, T. B. Clark and D. A. Watson, *J. Am. Chem. Soc.*, 2020, **142**, 11988–11992.
- 37 F. G. Mann and H. R. Watson, *J. Chem. Soc.*, 1957, 3945–3949.
- 38 F. Benvenuti, C. Carlini, M. Marchionna, R. Patrini, A. M. Raspolli Galletti and G. Sbrana, *J. Mol. Catal. A: Chem.*, 1999, **140**, 139–155.
- 39 R. J. Lundgren, B. D. Peters, P. G. Alsabeh and M. Stradiotto, *Angew. Chem., Int. Ed.*, 2010, **49**, 4071–4074.
- 40 W. Levason and K. G. Smith, *Inorg. Chim. Acta*, 1980, **41**, 133–141.
- 41 P. Espinet and K. Soulantica, *Coord. Chem. Rev.*, 1999, **193–195**, 499–556.
- 42 F. Speiser, P. Braunstein and L. Saussine, *Acc. Chem. Res.*, 2005, **38**, 784–793.
- 43 A. Kermagoret and P. Braunstein, *Organometallics*, 2008, **27**, 88–99.
- 44 H. Olivier-Bourbigou, P. A. R. Breuil, L. Magna, T. Michel, M. F. Espada Pastor and D. Delcroix, *Chem. Rev.*, 2020, **120**, 7919–7983.
- 45 G. E. Bekmukhamedov, A. V. Sukhov, A. M. Kuchkaev and D. G. Yakhvarov, *Catalysts*, 2020, **10**, 498.
- 46 F. Wang and C. Chen, *Polym. Chem.*, 2019, **10**, 2354–2369.
- 47 D. Zhang, E. T. Nadres, M. Brookhart and O. Daugulis, *Organometallics*, 2013, **32**, 5136–5143.
- 48 F. L. Grasset, R. Welter, P. Braunstein, H. Olivier-Bourbigou and L. Magna, *ChemCatChem*, 2021, **13**, 2167–2178.
- 49 J. Flapper, H. Kooijman, M. Lutz, A. L. Spek, P. W. N. M. van Leeuwen, C. J. Elsevier and P. C. J. Kamer, *Organometallics*, 2009, **28**, 3272–3281.
- 50 J. Flapper, P. W. N. M. van Leeuwen, C. J. Elsevier and P. C. J. Kamer, *Organometallics*, 2009, **28**, 3264–3271.
- 51 D. H. Camacho, E. V. Salo, J. W. Ziller and Z. Guan, *Angew. Chem., Int. Ed.*, 2004, **43**, 1821–1825.
- 52 P. W. N. M. van Leeuwen, P. C. J. Kamer, J. N. H. Reek and P. Dierkes, *Chem. Rev.*, 2000, **100**, 2741–2769.
- 53 K. Yamamoto, K. Higuchi, M. Ogawa, H. Sogawa, S. Kuwata, Y. Hayashi, S. Kawauchi and T. Takata, *Chem. – Asian J.*, 2020, **15**, 356–359.
- 54 L. Cao, Z. Cai and M. Li, *Macromolecules*, 2022, **55**, 3513–3521.

